Article

The Facile Generation of a Tetramethyleneethane Type Radical Cation and Biradical Utilizing a 3,4-Di(□-styryl)furan and a Photoinduced ET and Back ET Sequence

Teruyo Ikeda, Hiroshi Ikeda, Yasutake Takahashi, Masafumi Yamada, Kazuhiko Mizuno, Shozo Tero-Kubota, and Seigo Yamauchi

J. Am. Chem. Soc., **2008**, 130 (8), 2466-2472 • DOI: 10.1021/ja074000b

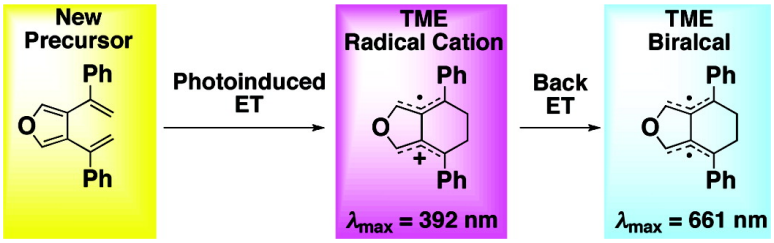

More About This Article

Additional resources and features associated with this article are available within the HTML version:

- Supporting Information
- Access to high resolution figures
- Links to articles and content related to this article
- Copyright permission to reproduce figures and/or text from this article

View the Full Text HTML

J|A|C|S
ARTICLES
Published on Web 02/01/2008

The Facile Generation of a Tetramethyleneethane Type Radical Cation and Biradical Utilizing a 3,4-Di(α-styryl)furan and a Photoinduced ET and Back ET Sequence

Teruyo Ikeda,[†] Hiroshi Ikeda,*[,‡] Yasutake Takahashi,[§] Masafumi Yamada,[†] Kazuhiko Mizuno,[‡] Shozo Tero-Kubota,[⊥] and Seigo Yamauchi[⊥]

Department of Chemistry, Graduate School of Science, Tohoku University, Sendai 980-8578, Japan, Department of Applied Chemistry, Graduate School of Engineering, Osaka Prefecture University, Sakai, Osaka 599-8531, Japan, Division of Chemistry, Graduate School of Medicine and Pharmaceutical Sciences, University of Toyama, 2630 Sugitani, Toyama 930-0194, Japan, and Institute of Multidisciplinary Research for Advanced Materials, Tohoku University, Sendai 980-8577, Japan

Received June 2, 2007; E-mail: ikeda@chem.osakafu-u.ac.jp

Abstract: Product analyses and nanosecond time-resolved spectroscopy on laser flash photolysis were studied for the photoinduced electron-transfer reaction of 3,4-di(α-styryl)furan (**6a**). A combination of these results, kinetic, density functional theoretical (DFT), and time-dependent DFT analyses enabled assignment of the absorption to the tetramethyleneethane (TME)-type radical cation (**7a**$^{\bullet+}$, λ_{max} = 392 nm) and the corresponding singlet biradical (^{1}**7a**$^{\bullet\bullet}$, λ_{max} = 661 nm). These two intermediates were mechanistically linked to each other with a facile back electron-transfer reaction. The present studies provide a new method for the generation of aryl-substituted TME-type intermediates.

Introduction

The tetramethyleneethane biradical (TME, **1**$^{\bullet\bullet}$, Chart 1)[1] is a prototypical non-Kekulé molecule. The main experimental[2] and theoretical[3] interest in this reactive intermediate is stimulated by an extraordinarily unique form of matter in terms of the electronic structure and multiplicity. The usual method employed to generate TME derivatives utilizes the photolytic or pyrolytic decomposition of diazo compounds. For example, the singlet state of 3,4-dimethylenefuran (**2**$^{\bullet\bullet}$),[2e,4] a furan analogue of TME with an absorption maximum (λ_{max}) at 560 nm, can be generated by photodeazetation of the diazene **3**.[4c] Especially, Berson and co-workers developed a series of 3,4-dimethylenefuran derivatives by using the photodeazetation and produced brilliant scientific achievements.[4] However, this approach for TME generation is limited by the fact that it is difficult to prepare the corresponding diazene precursors.

Chart 1

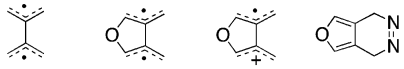

Ikeda and Miyashi previously reported that the photoinduced electron-transfer (PET) degenerate Cope rearrangement of 2,5-

[†] Department of Chemistry, Graduate School of Science, Tohoku University.
[‡] Osaka Prefecture University.
[§] University of Toyama.
[⊥] Institute of Multidisciplinary Research for Advanced Materials, Tohoku University.

(1) (a) Pittner, J.; Nachtigall, P.; Čársky, P. *J. Phys. Chem. A* **2001**, *105*, 1354−1356. (b) Rodríguez, E. R.; Reguero, M.; Caballol, R. *J. Phys. Chem. A* **2000**, *104*, 6253−6258. (c) Filatov, M.; Shaik, S. *J. Phys. Chem. A* **1999**, *103*, 8885−8889. (d) Nachtigall, P.; Jordan, K. D. *J. Am. Chem. Soc.* **1993**, *115*, 270−271. (e) Dowd, P.; Chang, W.; Partian, C. J.; Zang, W. *J. Phys. Chem.* **1993**, *97*, 13408−13412. (f) Nachtigall, P.; Jordan, K. D. *J. Am. Chem. Soc.* **1992**, *114*, 4743−4747. (g) Du, P.; Borden, W. T. *J. Am. Chem. Soc.* **1987**, *109*, 930−931. (h) Dowd, P.; Chang, W.; Paik, Y. H. *J. Am. Chem. Soc.* **1986**, *108*, 7416−7417. (i) Lahti, P. M.; Rossi, A. R.; Berson, J. A. *J. Am. Chem. Soc*. **1985**, *107*, 2273−2280. (j) Dowd, P. *J. Am. Chem. Soc*. **1970**, *92*, 1066−1068. (k) Dolbier, W. R., Jr. *Tetrahedron Lett.* **1968**, *4*, 393−396. (l) Longuet-Higgins, H. C. *J. Chem. Phys*. **1950**, *18*, 265−274.

(2) (a) Bangal, P. R.; Tamai, N.; Yokoyama, Y.; Tukada, H. *J. Phys. Chem. A* **2004**, *108*, 578−585. (b) Maier, G.; Senger, S. *Eur. J. Org. Chem*. **1999**, 1291−1294. (c) Matsuda, K.; Iwamura, H. *J. Chem. Soc., Perkin Trans. 2* **1998**, 1023−1026. (d) Matsuda, K.; Iwamura, H. *J. Am. Chem. Soc*. **1997**, *119*, 7412−7413. (e) Nash, J. J.; Dowd, P.; Jordan, K. D. *J. Am. Chem. Soc*. **1992**, *114*, 10071−10072. (f) Jelinek-Fink, H.; Christl, M.; Peters, E.-M.; Peters, K.; Schnering, G. v. *Chem. Ber*. **1991**, *124*, 2569−2575. (g) Dowd, P.; Chang, W.; Paik, Y. H. *J. Am. Chem. Soc.* **1987**, *109*, 5284−5285. (h) Bushby, R. J.; Mann, S.; Jesudason, M. V. *Tetrahedron Lett.* **1983**, *24*, 4743−4744. (i) Bauld, N. L.; Chang, C.-S. *J. Am. Chem. Soc.* **1972**, *94*, 7594−7595. (j) Gajewski, J. J.; Shih, C. N. *J. Am. Chem. Soc.* **1969**, *91*, 5900−5901.

(3) (a) Tukada, H.; Bangal, P. R.; Tamai, N.; Yokoyama, Y. *J. Mol. Struct. (Theochem)* **2005**, *724*, 215−219. (b) Datta, S. N.; Mukherjee, P.; Jha, P. P. *J. Phys. Chem. A* **2003**, *107*, 5049−5057. (c) Havlas, Z.; Michl, J. *J. Mol. Struct. (Theochem*) **1997**, *398*−*399*, 281−291. (d) Prasad, B. L. V.; Radhakrishnan, T. P. *J. Mol. Struct. (Theochem*) **1996**, *361*, 175−180. (e) Lahti, P. M.; Ichimura, A. S.; Berson, J. A. *J. Org. Chem.* **1989**, *54*, 958−965. (f) Choi, Y.; Jordan, K. D.; Paik, Y. H.; Chang, W.; Dowd, P. *J. Am. Chem. Soc*. **1988**, *110*, 7575−7576.

(4) (a) Heath, R. B.; Bush, L. C.; Feng, X.-W.; Berson, J. A.; Scaiano, J. C.; Berinstain, A. B. *J. Phys. Chem* **1993**, *97*, 13355−13357. (b) Greenberg, M. M.; Blackstock, S. C.; Berson, J. A.; Merrill, R. A.; Duchamp, J. C.; Zilm, K. W. *J. Am. Chem. Soc*. **1991**, *113*, 2318−2319. (c) Greenberg, M. M.; Blackstock, S. C.; Stone, K. J.; Berson, J. A. *J. Am. Chem. Soc*. **1989**, *111*, 3671−3679. (d) Scaiano, J. C.; Wintgens, V.; Haider, K.; Berson, J. A. *J. Am. Chem Soc.* **1989**, *111*, 8732−8733. (e) Scaiano, J. C.; Wintgens, V.; Bedell, A.; Berson, J. A. *J. Am. Chem. Soc*. **1988**, *110*, 4050−4051. (f) Zilm, K. W.; Merrill, R. A.; Greenberg, M. M.; Berson, J. A. *J. Am. Chem. Soc*. **1987**, *109*, 1567−1569. (g) Greenberg, M. M.; Blackstock, S. C.; Berson, J. A. *Tetrahedron Lett.* **1987**, 4263−4266. (h) Stone, K. J.; Greenberg, M. M.; Goodman, J. L.; Peters, K. S.; Berson, J. A. *J. Am. Chem. Soc*. **1986**, *108*, 8088−8089.

 10.1021/ja074000b CCC: $40.75

Scheme 1

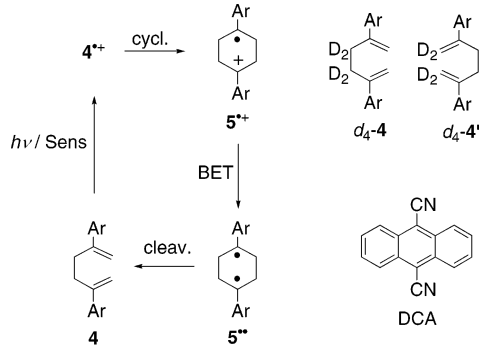

Scheme 2

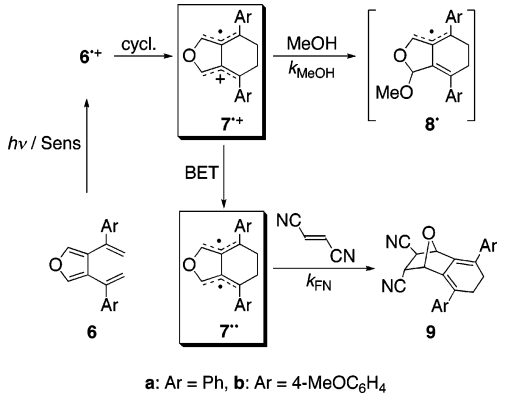

diaryl-1,5-hexadienes (**4**, Scheme 1) by using a tetradeuterio-labeled compound (d_4-**4** or d_4-**4′**) as a substrate and 9,10-dicyanoanthracene (DCA) as an electron-accepting photosensitizer (Sens) (Scheme 1).[5] The important key process of the mechanism is the highly exothermic back electron transfer (BET) from $DCA^{\bullet-}$ to 1,4-diarylcyclohexane-1,4-diyl radical cation (**5**$^{\bullet+}$), given by intramolecular cyclization of the initially formed **4**$^{\bullet+}$, to form 1,4-diarylcyclohexane-1,4-diyl biradical (**5**$^{\bullet\bullet}$). The existence of **5**$^{\bullet\bullet}$ was recently confirmed by thermoluminescence experiment,[6] while **5**$^{\bullet+}$ was observed with nanosecond time-resolved absorption spectroscopy on laser flash photolysis (LFP).[5a,e] Bauld[7a] and Williams[7b,c] also demonstrated an intramolecular cyclization processes of the 1,5-hexadiene unit triggered by one electron oxidation.

In the studies described below, we have uncovered a new method to generate TME-type radical cations and biradicals by using synthetically convenient methods that rely on intramolecular cyclization processes of the 1,5-hexadiene radical cation unit.[5,7] This is exemplified by the PET reactions of the 3,4-di(α-styryl)furan derivatives **6** (Scheme 2), in which the initially formed radical cations **6**$^{\bullet+}$ undergo cyclization to produce TME-type radical cations **7**$^{\bullet+}$. This is followed by BET from the sensitizer radical anion to give TME-type biradicals **7**$^{\bullet\bullet}$. This method not only represents a new approach to the generation of TME-type biradicals but also serves to generate a new TME-type of radical cation about which little is known,[8] namely, 3,4-dimethylenefuran radical cation (**2**$^{\bullet+}$). Below, we describe the results of product analyses, nanosecond time-resolved absorption spectroscopy on LFP of **6**, and preliminarily theoretical analyses of the electronic structure of **7**$^{\bullet+}$ and **7**$^{\bullet\bullet}$ using density functional theory (DFT).

Scheme 3 [a]

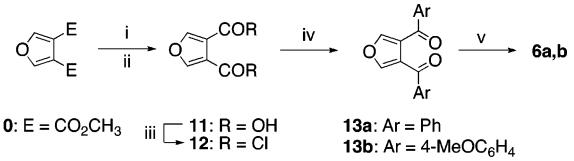

[a] Conditions: (i) $KOH/CH_3OH/H_2O$; (ii) HCl aq, yield, 100%; (iii) $SOCl_2$; (iv) $AlCl_3$/benzene for **12a**, yield, 85% from **11** or $AlCl_3$/anisole for **12b**, yield, 13% from **11**; (v) Ph_3PCH_3I/*t*-BuOK, THF, yield, 65% for **6a**, yield, 23% for **6b**.

Table 1. Oxidation Potentials ($E^{ox}_{1/2}$) and Free Energy Changes (ΔG_{ET}) of Electron-Transfer Reactions Associated with DCA* or $NMQ^+BF_4^-$*

conditions	$E^{ox}_{1/2}$[a] V	ΔG_{ET}(DCA)[b] eV	ΔG_{ET}($NMQ^+BF_4^-$)[b] eV
6a	+1.87	−0.34	−1.33
6b	+1.42	−0.79	−1.78

[a] Value vs SCE, 0.1 M *n*-$Bu_4N^+BF_4^-$ in CH_2Cl_2, platinum electrode, scan rate 100 mV s^{-1}, irreversible wave, $E^{ox}_{1/2} = E_{pa} - 0.03$ V. [b] $\Delta G_{ET} = E^{ox}_{1/2}$(**6**) − $E^{red}_{1/2}$(sens) − E_{0-0}(sens) − $e^2/\epsilon r$.[10] $E^{red}_{1/2}$(DCA) = −0.89 V vs SCE, E_{0-0}(DCA) = 2.87 eV, $E^{red}_{1/2}(NMQ^+BF_4^-)$ = −0.51 V vs SCE and $E_{0-0}(NMQ^+BF_4^-)$ = 3.48 eV; the coulomb term, $e^2/\epsilon r$, is +0.23 eV in CH_2Cl_2.

Results and Discussion

Syntheses and Electron Donating Properties. 3,4-Di(α-styryl)furan **6a** was prepared from acid chloride **12** by Friedel−Crafts reaction followed by Wittig olefination of 3,4-dibenzoylfuran (**13a**, Scheme 3). Compound **12** was obtained from dimethyl 3,4-furandicarboxylate (**10**). The anisyl derivative **6b** was prepared from the corresponding furan **13b** using the same method.

Furans **6a** and **6b** are relatively good electron donors and their oxidation potentials ($E^{ox}_{1/2}$) in CH_2Cl_2 are low enough to quench the excited singlet state of DCA and *N*-methylquinolinium tetrafluoroborate ($NMQ^+BF_4^-$)[9] exothermically (Table 1). Free energy changes (ΔG_{ET}) associated with the forward electron transfer are all negative as calculated according to the Rehm−Weller equation.[10] In accord with calculated thermody-

(5) (a) Miyashi, T.; Ikeda, H.; Takahashi, Y. *Acc. Chem. Res.* **1999**, *32*, 815−824. (b) Ikeda, H.; Takasaki, T.; Takahashi, Y.; Konno, A.; Matsumoto, M.; Hoshi, Y.; Aoki, T.; Suzuki, T.; Goodman, J. L.; Miyashi, T. *J. Org. Chem.* **1999**, *64*, 1640−1649. (c) Ikeda, H.; Minegishi, T.; Abe, H.; Konno, A.; Goodman, J. L.; Miyashi, T. *J. Am. Chem. Soc.* **1998**, *120*, 87−95. (d) Ikeda, H.; Ishida, A.; Takasaki, T.; Tojo, S.; Takamuku, S.; Miyashi, T. *J. Chem. Soc., Perkin Trans. 2* **1997**, *5*, 849−850. (e) Ikeda, H.; Minegishi, T.; Takahashi, Y.; Miyashi, T. *Tetrahedron Lett.* **1996**, *37*, 4377−4380. (f) Miyashi, T.; Takahashi, Y.; Ohaku, H.; Ikeda, H.; Morishima, S.-i. *Pure Appl. Chem.* **1991**, *63*, 223−230. (g) Miyashi, T.; Ikeda, H.; Konno, A.; Okitsu, O.; Takahashi, Y. *Pure Appl. Chem.* **1990**, *62*, 1531−1538. (h) Miyashi, T.; Konno, A.; Takahashi, Y. *J. Am. Chem. Soc.* **1988**, *110*, 3676−3677.
(6) (a) Namai, H.; Ikeda, H.; Hoshi, Y.; Mizuno, K. *Angew. Chem., Int. Ed.* **2007**, *46*, 7396−7398. (b) Namai, H.; Ikeda, H.; Hoshi, Y.; Kato, N.; Morishita, Y.; Mizuno, K. *J. Am. Chem. Soc.* **2007**, *129*, 9032−9036.
(7) (a) Lorenz, K.; Bauld, N. L. *J. Catal.* **1985**, *95*, 613−616. (b) Williams, F.; Guo, Q.-X.; Bebout, D. C.; Carpenter, B. K. *J. Am. Chem. Soc.* **1989**, *111*, 4133−4134. (c) Guo, Q.-X.; Qin, X.-Z.; Wang, J. T.; Williams, F. *J. Am. Chem. Soc.* **1988**, *110*, 1974−1976.
(8) (a) Norberg, D.; Larsson, P.-E.; Dong, X.-C.; Salhi-Benachenhou, N.; Lunell, S. *Int. J. Quantum Chem.* **2004**, *98*, 473−483. (b) Ikeda, H.; Tanaka, F.; Akiyama, K.; Tero-Kubota, S.; Miyashi, T. *J. Am. Chem. Soc.* **2004**, *126*, 414−415. (c) Müller, B.; Bally, T.; Gerson, F.; Meijere, A. d.; Seebach, M. v. *J. Am. Chem. Soc.* **2003**, *125*, 13776−13783. (d) Gerson, F.; Schmidlin, R.; Meijere, A. d.; Späth, T. *J. Am. Chem. Soc.* **1995**, *117*, 8431−8434. (e) Gerson, F.; Meijere, A. d.; Qin, X.-Z. *J. Am. Chem. Soc.* **1989**, *111*, 1135−1136.
(9) Yoon, U. C.; Quillen, S. L.; Mariano, P. S.; Swanson, R.; Stavinoha, J. L.; Bay, E. *J. Am. Chem. Soc.* **1983**, *105*, 1204−1218.
(10) Rehm, D.; Weller, A. *Isr. J. Chem.* **1970**, *8*, 259−271.

Table 2. The DCA-Sensitized Photoreactions of **6a**[a] with Diylophiles

diylophile	time (h)	product	yield (%)
FN	1.5	**9a**	96
DMDCF	3.5	**14a**	84
MA	2	**15a**	92 (*exo:endo* = 65:35)
DMF[b]	2	**16a**	98 (*trans*)
DMM	3	**16a**	63 (*exo, cis:endo, cis* = 85:15)

[a] A 5 mL solution in a test tube was irradiated with a 2 kW Xe lamp through a cutoff filter (Toshiba L-39, $\lambda > 360$ nm) at room temperature: [**6a**] = 0.04 M, [DCA] = 1 mM, [diylophile] = 0.08 M in CH_2Cl_2. [b] [DMF] = 0.12 M.

Chart 2

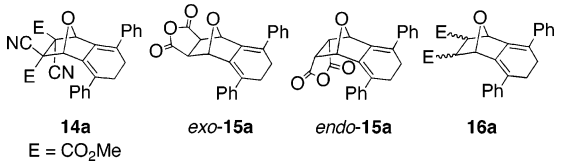

namics, the DCA fluorescence was efficiently quenched by **6a** and **6b** in CH_2Cl_2 with large rate constants ($k_q > 0.9 \times 10^{10}$ M^{-1} s^{-1}) close to the diffusion-control rate.

Photoinduced Electron-Transfer Reaction. Irradiation (2 kW Xe lamp, $\lambda > 360$ nm) of a degassed CH_2Cl_2 solution containing DCA and **6a** led to the formation of a complex product mixture. When this photoreaction was carried out in the presence of fumaronitrile (FN) as a trapping agent, the [4 + 2] type cycloadduct **9a** was produced in a 96% yield (Table 2). In a similar manner, PET reactions of **6a** in the presence of dimethyl dicyanofumarate (DMDCF), maleic anhydride (MA), dimethyl fumarate (DMF), and dimethyl maleate (DMM) gave the respective adducts **14a**, **15a**, and **16a** in high yields (Chart 2). The results strongly suggest the PET reaction of **6a** in which **7a**$^{\bullet\bullet}$ serves as an intermediate. In addition, the observation that reaction of **7a**$^{\bullet\bullet}$ with DMM took place with stereochemical retention suggests that the [4 + 2] type cycloaddition reaction occurs in a concerted manner.

Laser Flash Photolysis. Nanosecond time-resolved absorption spectroscopy on LFP was used to observe the reactive intermediates, **7**$^{\bullet+}$ and **7**$^{\bullet\bullet}$ that participate in this pathway (Scheme 2). Under $NMQ^+BF_4^-$−toluene/CH_3CN conditions which reduce the efficiency of BET,[11] LFP of **6a** or its anisyl analogue **6b** gave rise to transient absorption bands with λ_{max} = 392 nm (Figure 1a, Table 3) or 448 nm, respectively. In contrast, under the DCA/CH_2Cl_2 conditions, LFP of **6a** or **6b** produced the respective transient absorption bands at 661 nm (Figure 1b) or 665 nm. On the basis of their analogy to that of the parent TME biradical (**2**$^{\bullet\bullet}$, vide supra) along with kinetic analyses and quantum calculations (vide infra), these absorption bands are assigned to **7a**$^{\bullet\bullet}$ and **7b**$^{\bullet\bullet}$ with the singlet multiplicity (^{1}**7a**$^{\bullet\bullet}$ and ^{1}**7b**$^{\bullet\bullet}$).

It is interesting that the rate constant for decay (k_d) of the 392-nm band associated with **7a**$^{\bullet+}$, formed under $NMQ^+BF_4^-$−toluene/CH_3CN conditions, was not dependent upon the concentration of FN but that it increased in a linear manner with an increase with the concentration of MeOH [k_{MeOH}(**7a**$^{\bullet+}$) = 5.3×10^5 M^{-1} s^{-1}].[12] In contrast, k_d associated with the 661-nm band of **7a**$^{\bullet\bullet}$ increased linearly with FN concentration [k_{FN}(**7a**$^{\bullet\bullet}$) = 1.1×10^7 M^{-1} s^{-1}] while decay of **7a**$^{\bullet\bullet}$, formed under DCA-sensitized conditions, was not affected by MeOH. Similar observations were made in the LFP studies with **6b** (Table 3). These complementary results strongly support our assignments for LFP experiments.

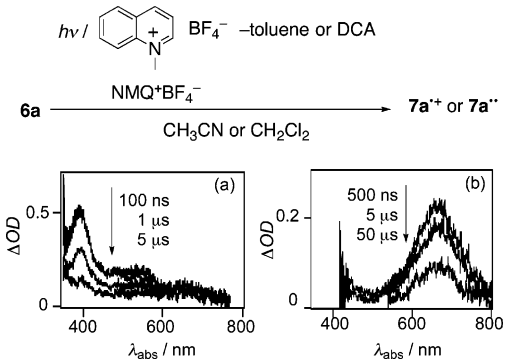

Figure 1. Transient absorption spectra obtained by LFP of **6a** under (a) $NMQ^+BF_4^-$−toluene/CH_3CN- and (b) DCA/CH_2Cl_2-sensitized conditions.

Table 3. Absorption Maxima (λ_{max}) of Transients Observed on LFP of **6**, Rate Constants for FN (k_{FN}) and MeOH (k_{MeOH}) Addition, and Assignment for Transients

conditions	λ_{max} nm	k_{FN}[a] $M^{-1}s^{-1}$	k_{MeOH}[a] $M^{-1}s^{-1}$	assignment
6a/$NMQ^+BF_4^-$−toluene/CH_3CN	392	*b*	5.3×10^5	**7a**$^{\bullet+}$
6b/$NMQ^+BF_4^-$−toluene/CH_3CN	448	*b*	5.1×10^4	**7b**$^{\bullet+}$
6a/DCA/CH_2Cl_2	661	1.1×10^7	*b*	^{1}**7a**$^{\bullet\bullet}$
6b/DCA/CH_2Cl_2	665	3.0×10^7	*b*	^{1}**7b**$^{\bullet\bullet}$

[a] At room temperature. [b] Not determined because of no reaction.

Chart 3

a: Ar = Ph, **b**: Ar = 4-$MeOC_6H_4$

The rate constant k_{MeOH}(**7a**$^{\bullet+}$) is lower than k_{MeOH} of **5a**$^{\bullet+}$ [$(6-8) \times 10^8$ M^{-1} s^{-1}][5c] and an axial, axial-chair conformer of the 1,4-diphenyl-2,3-dimethylcyclohexa-1,4-diyl radical cation [*aaC*-**17a**$^{\bullet+}$ in Chart 3, $(5.6-8.8) \times 10^8$ M^{-1} s^{-1}].[5b] Similarly, k_{MeOH}(**7b**$^{\bullet+}$) is lower than k_{MeOH} of *aaC*-**17b**$^{\bullet+}$ [$(7.1-8.5) \times 10^5$ M^{-1} s^{-1}].[5b] These results suggest that a positive charge delocalizes effectively in the conjugated system bridged by an oxygen atom. In addition, the parent diyl **2**$^{\bullet\bullet}$ is known to react with FN to give adduct **18** with a rate constant k_{FN}(**2**$^{\bullet\bullet}$) of 3.2×10^8 M^{-1} s^{-1} (295 K).[4a] The fact that k_{FN}(**7a**$^{\bullet\bullet}$) is smaller than k_{FN}(**2**$^{\bullet\bullet}$) suggests that spin delocalization in the more conjugated present system slows the trapping reaction (vide infra).

DFT Calculation. Theoretical calculation is essential to elucidate the molecular geometry and electronic structure today. DFT calculation often gives satisfactory results.[13] Stephens and

(11) (a) Ikeda, H.; Hoshi, Y.; Namai, H.; Tanaka, F.; Goodman, J. L.; Mizuno, K. *Chem. Eur. J.* **2007**, *13*, 9207−9215. (b) Ikeda, H.; Akiyama, K.; Takahashi, Y.; Nakamura, T.; Ishizaki, S.; Shiratori, Y.; Ohaku, H.; Goodman, J. L.; Houmam, A.; Wayner, D. D. M.; Tero-Kubota, S.; Miyashi, T. *J. Am. Chem. Soc.* **2003**, *125*, 9147−9157.

(12) In this reaction, the intermediacy of **8a**$^{\bullet}$ is predicted, though any obvious MeOH adduct was not isolated. When a similar PET reaction was subjected for **4a** or 1,4-diphenyl-2,3-diazabicylo[2.2.0]hexane in CH_2Cl_2 containing MeOH and chloranil as a sensitizer, two MeOH−adducts, *syn*- and *anti*-1,4-dimethoxy-1,4-diphenylcyclohexanes, were isolated in low yields. (Minegishi, T. Doctor Thesis. Tohoku University: Sendai, Japan, 1997.)

(13) (a) Eriksson, L. A.; Malkin, V. G.; Malkina, O. L.; Salahub, D. R. *Int. J. Quantum Chem.* **1994**, *52*, 879−901. (b) Eriksson, L. A.; Malkin, V. G.; Malkina, O. L.; Salahub, D. R. *J. Chem. Phys.* **1993**, *99*, 9756−9763.

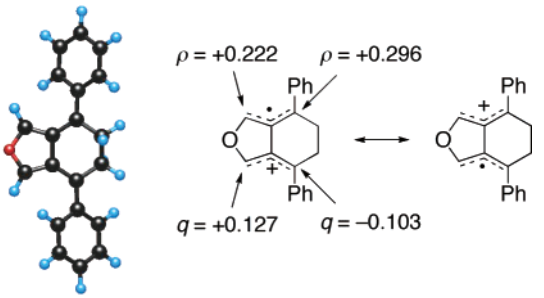

Figure 2. Optimized molecular geometry and the selected charge and spin densities (q and ρ, respectively) of **7a**$^{\bullet+}$ calculated using UB3LYP/cc-pVDZ.

co-workers reported[14] that DFT/B3LYP [Becke's hybrid, three-parameter functional[15] and the nonlocal correlation functional of Lee, Yang, and Parr[16]] force field gave satisfactory results of the vibrational absorption and circular dichromism spectra, as compared with self-consistent field (SCF) or the second-order Møller−Plesset perturbation theory (MP2)[17] force field. Indeed in our experience, charge and spin densities (q and ρ, respectively) calculated with DFT/B3LYP method are good enough to explain the reactivity of 2,2′,3,3′-tetraphenylbicyclopropenyl radical cations [ROB3LYP/6-31G(p)],[18] the molecular geometry and electronic structure of the geminally diphenyl-substituted trimethylenemethane radical cation (UB3LYP/cc-pVDZ)[19] and 1,4-diphenylcyclohexane-1,4-diyl radical cation (**5a**$^{\bullet+}$, UB3LYP/cc-pVDZ),[11a] classical and nonclassical radical ions derived from 7-benzhydrylidenenorbornene analogues,[20] and others.[21]

To elucidate the molecular geometry and electronic structure, we examined DFT[22] calculations for **7a**$^{\bullet+}$ and **7a**$^{\bullet\bullet}$. Figure 2 shows a nearly planar molecular geometry of **7a**$^{\bullet+}$ optimized using UB3LYP/cc-pVDZ. The calculated charge densities q at the two terminal carbons of allyl cation unit are +0.127 and −0.103, respectively, suggesting a regioselective nucleophilic attack of MeOH to **7a**$^{\bullet+}$ to give a possible adduct, **8a**$^{\bullet}$. Similarly, the spin densities ρ at the two terminal carbons of allyl radical unit are calculated to be +0.222 and +0.296, respectively, which are less than those of ^{1}**7a**$^{\bullet\bullet}$ (vide infra).

A similar molecular geometry was suggested for ^{1}**7a**$^{\bullet\bullet}$ (Figure 3b, vide infra) and ^{3}**7a**$^{\bullet\bullet}$. Information about the multiplicity of the ground state of **7a**$^{\bullet\bullet}$ has come from the relative total energy

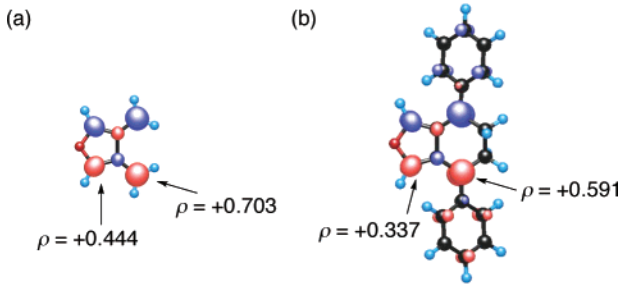

Figure 3. The selected spin densities (ρ) of (a) ^{1}**2**$^{\bullet\bullet}$ and (b) ^{1}**7a**$^{\bullet\bullet}$ on the optimized structures calculated using UB3LYP/cc-pVDZ.

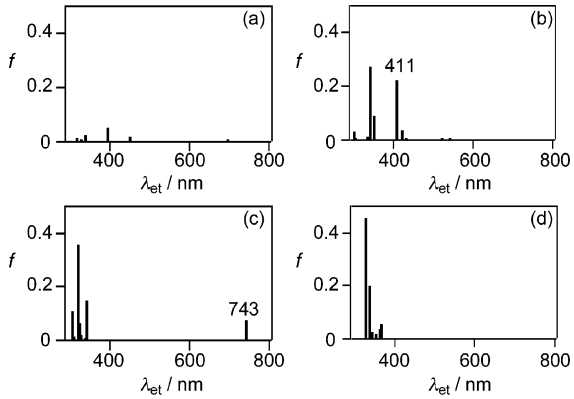

Figure 4. Electronic transitions of (a) **6a**$^{\bullet+}$, (b) **7a**$^{\bullet+}$, (c) ^{1}**7a**$^{\bullet\bullet}$, and (d) ^{3}**7a**$^{\bullet\bullet}$ calculated using TD-UB3LYP/cc-pVDZ.

corrected with the zero-point energy (ΔE) of ^{1}**7a**$^{\bullet\bullet}$ and ^{3}**7a**$^{\bullet\bullet}$, which were computed to be ΔE(^{1}**7a**$^{\bullet\bullet}$) = 0.38 eV and ΔE(^{3}**7a**$^{\bullet\bullet}$) = 0.47 eV, relative to the ground state of **6a** (0 eV) by using DFT calculations at the (U)B3LYP/cc-pVDZ level. Thus, the singlet−triplet gap for **7a**$^{\bullet\bullet}$ is estimated to be ca. 0.09 eV. Unfortunately, however, this value is not accurate judging from the total spin S^2 of **7a**$^{\bullet\bullet}$. In our case, spin contamination is negligible for ^{3}**7a**$^{\bullet\bullet}$ (S^2 = 2.0012 while $\langle S^2\rangle$ = 2 for pure triplet) but not for ^{1}**7a**$^{\bullet\bullet}$ (S^2 = 0.3767 for $\langle S^2\rangle \approx 0$ for pure singlet, but not = 0 at this method because of its open shell character). Therefore, the ΔE(^{1}**7a**$^{\bullet\bullet}$) of 0.38 eV is overestimated while the singlet−triplet gap of 0.09 eV is underestimated. With S^2 = 0.3767, ^{1}**7a**$^{\bullet\bullet}$ is assumed to be a 81:19 mixture of pure singlet ($\langle S^2\rangle \approx 0$) and triplet ($\langle S^2\rangle$ = 2). Therefore, the actual singlet−triplet gap and ΔE(^{1}**7a**$^{\bullet\bullet}$) is estimated to be *ca.* 0.11 (0.09/0.81) and *ca.* 0.36 (0.47 − 0.11) eV, respectively. A comparison of the spin densities ρ at the two terminal carbons of allyl radical unit in ^{1}**2**$^{\bullet\bullet}$ and ^{1}**7a**$^{\bullet\bullet}$ (Figure 3) shows that odd electrons in ^{1}**7a**$^{\bullet\bullet}$ are distributed into both the TME system and the phenyl groups.

The time-dependent (TD) DFT calculations show that the electronic transition of **7a**$^{\bullet+}$ should have an oscillator strength (f) at λ_{et} = 411 nm (Figure 4b) that is larger than that of **6a**$^{\bullet+}$ (Figure 4a). Thus, it appears that the 392-nm band (Figure 1a) originates from **7a**$^{\bullet+}$ rather than **6a**$^{\bullet+}$. The calculated electronic transition for ^{1}**7a**$^{\bullet\bullet}$ and ^{3}**7a**$^{\bullet\bullet}$ afforded contrastive results (Figure 4c and 4d). With electrons of the same spin in the two nonbonding orbitals, ^{3}**7a**$^{\bullet\bullet}$ should not have any low-lying excited states. Indeed, our TDDFT calculations on the triplet find no transitions predicted above 400 nm (Figure 4d). Therefore, ^{3}**7a**$^{\bullet\bullet}$ cannot be the species that absorbs at long wavelengths. In contrast, in ^{1}**7a**$^{\bullet\bullet}$ the two electrons in the nonbonding orbitals have opposite spin. Consequently, excitation of an electron from one nonbonding orbital into the other is possible in the singlet;

(14) Stephens, P. J.; Devlin, F. J.; Chabalowski, C. F.; Frisch, M. J. *J. Phys. Chem.* **1994**, *98*, 11623−11627.
(15) Becke, A. D. *J. Chem. Phys.* **1993**, *98*, 5648−5652.
(16) Lee, C.; Yang, W.; Parr, R. G. *Phys. Rev. B* **1988**, *37*, 785−789.
(17) It is reported that MP2 overestimates spin densities on carbon significantly for some systems; see: (a) Krogh-Jespersen, K.; Roth, H. D. *J. Am. Chem. Soc.* **1992**, *114*, 8388−8394. (b) Raghavachari, K.; Roth, H. D. *J. Am. Chem. Soc.* **1989**, *111*, 7132−7136. (c) Roth, H. D.; Schilling, M. L. M.; Raghavachari, K. *J. Am. Chem. Soc.* **1984**, *106*, 253−255. (d) Raghavachari, K.; Haddon, R. C.; Roth, H. D. *J. Am. Chem. Soc.* **1983**, *105*, 3110−3114.
(18) Ikeda, H.; Hoshi, Y.; Kikuchi, Y.; Tanaka, F.; Miyashi, T. *Org. Lett.* **2004**, *6*, 1029−1032.
(19) Namai, H.; Ikeda, H.; Kato, N.; Mizuno, K. *J. Phys. Chem. A* **2007**, *111*, 4436−4442.
(20) (a) Namai, H.; Ikeda, H.; Hirano, T.; Ishii, H.; Mizuno, K. *J. Phys. Chem. A* **2007**, *111*, 7898−7905. (b) Ikeda, H.; Namai, H.; Hirano, T. *Tetrahedron Lett.* **2005**, *46*, 3917−3921. (c) Ikeda, H.; Namai, H.; Hirano, T. *Tetrahedron Lett.* **2005**, *46*, 7631−7635.
(21) (a) Ikeda, H.; Namai, H.; Kato, N.; Ikeda, T. *Tetrahedron Lett.* **2006**, *47*, 1857−1860. (b) Ikeda, H.; Namai, H.; Kato, N.; Ikeda, T. *Tetrahedron Lett.* **2006**, *47*, 1501−1504. (c) Ikeda, H.; Tanaka, F.; Kabuto, C. *Tetrahedron Lett.* **2005**, *46*, 2663−2667. (d) Ikeda, H.; Tanaka, F.; Miyashi, T.; Akiyama, K.; Tero-Kubota, S. *Eur. J. Org. Chem.* **2004**, 1500−1508.
(22) DFT calculation were performed using the program Gaussian 98.[23] Figures 2 and 3 were drawn using the WinMOPAC 3.9 software.[24]
(23) Frisch, M. J.; et al. *Gaussian 98*, revision A.11.4; Gaussian, Inc.: Pittsburgh, PA, 1998.
(24) *WinMOPAC*, version 3.9; Fujitsu Ltd.: Tokyo, Japan, 2004.

Scheme 4

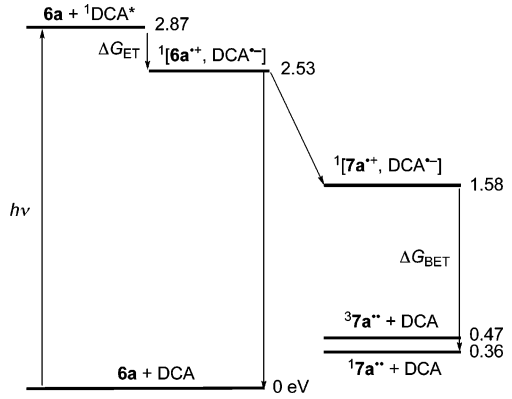

[a] A plalusible energy diagram for DCA-sensitized PET reaction of **6a** in CH_2Cl_2. Values of the relative energy are shown.

Chart 4

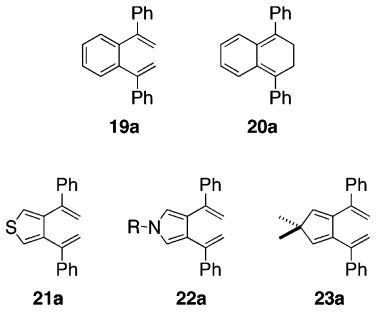

so a long wavelength electronic absorption is expected for ^{1}**7a••**. Although the value of $S^2 = 0.3767$ for the UB3LYP wave function for ^{1}**7a••** makes TDDFT calculations unlikely to give quantitatively reliable results for this state, it is worth noting that our TDDFT calculations do predict a long wavelength absorption at 743 nm for ^{1}**7a••** (Figure 4c). Therefore, from the combined experimental and calculation results, ^{1}**7a••** is much more likely than ^{3}**7a••** to be the species with the long wavelength absorption that we observe experimentally (Figure 1b).

Estimate of the Rate Constant for BET Yielding TME ^{1}7a••. Finally, an estimate of the free energy changes in BET (ΔG_{BET}) from DCA$^{\bullet-}$ to **7a**$^{\bullet+}$ to give ^{1}**7a••** was calculated to be −1.22 eV. This value was obtained by analyses of an energy diagram (Scheme 4) for the DCA-sensitized PET reaction of **6a** in CH_2Cl_2. After excitation of DCA (2.87 eV), electron transfer from **6a** to ^{1}DCA* with $\Delta G_{ET} = -0.34$ eV gives a radical ion pair ^{1}[**6a**$^{\bullet+}$, DCA$^{\bullet-}$] with the energy of 2.53 eV. Then, a facile cyclization, competing with BET giving the starting materials, occurs exothermically to give another radical ion pair ^{1}[**7a**$^{\bullet+}$, DCA$^{\bullet-}$] with 1.58 eV. This value was estimated as the difference in the total energy between **6a**$^{\bullet+}$ and **7a**$^{\bullet+}$, using (U)B3LYP/cc-pVDZ. A facile BET from DCA$^{\bullet-}$ to **7a**$^{\bullet+}$ finally affords ^{1}**7a••** with the calculated energy of 0.36 eV (vide supra). Therefore, the difference in energy between ^{1}[**7a**$^{\bullet+}$, DCA$^{\bullet-}$] and ^{1}**7a••** + DCA affords $\Delta G_{BET} = -1.22$ eV.[25]

The value of −1.22 eV, when used in the eqs 1 and 2,[26] enabled an estimate of the rate constant for BET from DCA$^{\bullet-}$ to **7a**$^{\bullet+}$ in a radical ion pair [**7a**$^{\bullet+}$, DCA$^{\bullet-}$], at 20 °C in CH_2Cl_2. The parameters in these equations were those suggested by Kikuchi and co-workers[27] [i.e., the electronic coupling matrix element V (18 cm^{-1}), solvent reorganization energy λ_s (1.00 eV), vibration reorganization energy λ_v (0.3 eV), single average frequency ν (1500 cm^{-1})] and Planck constant h, Boltzmann constant k_b, and the temperature T (293 K), respectively. This calculation gave an estimated k_{BET} of 5.9×10^{10} s^{-1}, which corresponds to values in the top region of a bell-shaped curve of k_{BET} versus ΔG_{BET}, suggesting efficient BET reaction.

$$k_{BET} = \left(\frac{4\pi^3}{h^2\lambda_s k_b T}\right)^{1/2} |V|^2 \sum_{\omega=0}^{\infty} \left(\frac{e^{-S}S^{\omega}}{\omega!}\right) \times \exp\left[-\frac{(\lambda_s + \Delta G_{BET} + \omega h\nu)^2}{4\lambda_s k_b T}\right] \quad (1)$$

$$S = \lambda_v / h\nu \quad (2)$$

Unfortunately, at present, this estimate of k_{BET} has not been checked experimentally yet. However, we have succeeded in checking experimentally similar estimate of k_{BET} in the PET intramolecular cyclization of benzene analogue **19a** (Chart 4).[28] We recently reported a preliminary result of spectroscopic and kinetic analyses of *o*-quinodimethane radical cation **20a**$^{\bullet+}$ and *o*-quinodimethane **20a** that is mechanistically connected with **20a**$^{\bullet+}$. These analyses confirmed for the first time that the decay rate constant of a *reactive* radical cation intervening in chemical reaction agrees with the rise rate constant of the corresponding reduced species formed by BET. We believe that similar BET process must operate in the PET reaction of **6** that includes **7**$^{\bullet+}$ and **7••**.

Conclusion

The results described above demonstrate that the PET reaction of **6** generates TME type reactive radical cations **7**$^{\bullet+}$ and the corresponding biradicals ^{1}**7••**. A key step for the conversion of **7**$^{\bullet+}$ to ^{1}**7••** is BET[29] from the sensitizer radical anion to **7**$^{\bullet+}$. These transients were characterized by using nanosecond time-resolved absorption spectroscopy on LFP and DFT calculations. Moreover, the generation of ^{1}**7••** is supported (1) by product analyses which show that PET reaction of **6a** with diylophiles yields characteristic [4 + 2] adducts and (2) by kinetic analyses of the decay of **7a**$^{\bullet+}$ and ^{1}**7a••** in the presence of MeOH and FN, respectively. The PET reaction of **6** involves an intramolecular cyclization reaction[5,7] that is similar to that taking place in the benzene analogue **19a**[28] even though the nature of the products generated in the PET reactions of these substrates are quite different. Specifically, it is quite interesting that **19a** gives rise to *o*-quinodimethane **20a**, a Kekulé-type product, while **6** yields the non-Kekulé type reactive intermediate **7••**.

The parent 3,4-dimethylenefuran **2••** and its analogues are known to have a very small single−triplet gap.[2d] The singlet−triplet gap for **7••** was also estimated to be only 0.11 eV with

(25) For the detail, see the Supporting Information.
(26) (a) Miller, J. R.; Beitz, J. V.; Huddleston, R. K. *J. Am. Chem. Soc.* **1984**, *106*, 5057−5068. (b) Siders, P.; Marcus, R. A. *J. Am. Chem. Soc.* **1981**, *103*, 741−747. (c) Siders, P.; Marcus, R. A. *J. Am. Chem. Soc.* **1981**, *103*, 748−752. (d) Van Duyne, R. P.; Fischer, S. F. *Chem. Phys.* **1974**, *5*, 183−197. (e) Ulstrup, J.; Jortner, J. *J. Chem. Phys.* **1975**, *63*, 4358−4368.
(27) Niwa, T.; Kikuchi, K.; Matsusita, N.; Hayashi, M.; Katagiri, T.; Takahashi, Y.; Miyashi, T. *J. Phys. Chem.* **1993**, *97*, 11960−11964.
(28) (a) Ikeda, H.; Ikeda, T.; Akagi, M.; Namai, H.; Miyashi, T.; Takahashi, Y.; Kamata, M. *Tetrahedron Lett.* **2005**, 1831−1835. (b) Takahashi, Y.; Ohya, Y.; Ikeda, H.; Miyashi, T. *J. Chem. Soc., Chem. Commun.* **1995**, 1749−1750.
(29) Marcus, R. A. *Ann. Rev. Phys. Chem.* **1964**, *15*, 155−196.

DFT calculation and careful consideration to the spin contamination in ^{1}**7a**$^{\bullet\bullet}$.[30] Our TDDFT calculation of ^{1}**7a**$^{\bullet\bullet}$ may not be accurate because of spin contamination. However, the conclusion that the ground state of **7a**$^{\bullet\bullet}$ is the singlet is still adequate by a process of elimination. Note that the TDDFT calculation of the pure triplet state ^{3}**7a**$^{\bullet\bullet}$ cannot explain the observed transient absorption spectra of **7a**$^{\bullet\bullet}$.

The results serve as the foundation of a new method to produce a variety of aryl-substituted TME radical cations and biradicals and to analyze their properties. As a matter of fact, we also studied similar PET reactions of thiophene, pyrrole, and 5,5-dimethyl-1,3-cyclopentadiene analogues (Chart 4, **21a**−**23a**) of **6**; the results will be reported elsewhere. As compared to trimethylenemethane,[31] TME has not been used very much for applications. Therefore, our results provide meaningful information not only for pure TME chemistry but also for the molecular design of TMEs for many applications, such as in organic syntheses and molecular devices, where the TME framework can be used as a building block of functionalized organic materials.

Experimental Section

General Methods. All melting points are uncorrected. Elemental analyses were performed by the Research and Analytical Center for Giant Molecules, Graduate School of Science, Tohoku University. ^{1}H NMR spectra were recorded at 200 MHz on a Varian Gemini 2000. ^{13}C NMR spectra were obtained at 50 MHz on a Varian Gemini 2000. Mass spectrometry (MS) was performed on a Hitachi M-2500 mass spectrometer with electron impact. Steady-state photolysis was carried out at 20 ± 1 °C using an Ushio 2-kW Xe short arc lamp through an aqueous IR filter and a Toshiba L-39 cutoff filter (λ > 360 nm) for DCA. CH_3CN was dried and distilled successively from P_2O_5 and CaH_2. CH_2Cl_2 was dried and distilled from CaH_2.

Physical Data of 6, 9, and 14−16. 6a. Colorless cubes (*n*-hexane), mp 82−84 °C. ^{1}H NMR (200 MHz, $CDCl_3$): δ_{ppm} 5.24 (s, 4 H), 7.1−7.2 (m, 10 H), 7.41 (s, 2 H). ^{13}C NMR (50 MHz, $CDCl_3$): δ_{ppm} 114.8 (2 C), 126.2 (2 C), 127.2 (4 C), 127.5 (4 C), 127.9 (2 C), 140.3 (2 C), 140.4 (2 C), 142.1 (2 C); IR (KBr) ν 3150, 3100, 3050, 1600, 1570, 1530, 1490, 1445, 1320, 1300, 1220, 1200, 1140, 1120, 1080, 1055, 1025, 900, 895, 880, 830, 810, 780, 775 cm^{-1}. MS (25 eV) *m*/*z* (relative intensity/%): 273 (M^+ + 1, 15), 272 (M^+, 100), 243 (33), 181 (21), 165 (52), 91 (17). Anal. Calcd for $C_{20}H_{16}O$: C, 88.20; H, 5.92. Found: C, 88.06; H, 6.06.

6b. Pale yellow solid (*n*-hexane), mp 79−80 °C. ^{1}H NMR (200 MHz, $CDCl_3$): δ_{ppm} 3.79 (s, 6 H), 5.16 (d, J = 1.6 Hz, 4 H), 6.73 (AA'BB', J = 8.9 Hz, 4 H), 7.11 (AA'BB', J = 8.9 Hz, 4 H), 7.41 (s, 2 H); ^{13}C NMR (50 MHz, $CDCl_3$) δ_{ppm} 55.2 (2 C), 113.2 (4 C), 126.4 (4 C), 128.3 (4 C), 133.1 (2 C), 139.6 (2 C), 142.0 (2 C), 159.2 (2 C). IR (KBr): ν 1603, 1578, 1533, 1508, 1458, 1394, 1304, 1178, 1138, 1113, 1022, 841, 750 cm^{-1}. MS (70 eV) *m*/*z* (relative intensity/%): 332 (M^+, 100), 303 (14), 224 (13), 211 (14), 172, (14), 121 (19). Anal. Calcd for $C_{22}H_{20}O_3$: C, 79.50; H, 6.07. Found: C, 79.30; H, 6.12.

9a. Colorless powder (CH_2Cl_2−ether), mp 210−212 °C. ^{1}H NMR (200 MHz, $CDCl_3$): δ_{ppm} 2.8−2.9 (m, 4 H), 3.30 (d, J = 4.4 Hz, 1 H), 3.44 (dd, J = 4.8, 4.4 Hz, 1 H), 5.53 (s, 1 H), 5.57 (d, J = 4.8 Hz, 1 H), 7.2−7.5 (m, 10 H). ^{13}C NMR (50 MHz, $CDCl_3$) δ_{ppm} 28.3, 28.6, 38.0, 39.2, 79.0, 81.6, 116.8, 118.0, 126.6 (2 C), 126.7 (2 C), 128.1, 128.2, 128.7 (2 C), 128.8, 129.0 (2 C), 131.1, 131.4, 132.4, 138.7, 139.1. IR (KBr): ν 3400, 3050, 2950, 2850, 2800, 2230, 1600, 1495, 1460, 1365, 1310, 1275, 1185, 1165, 1025, 1010, 960, 925, 905, 850, 815, 760, 755 cm^{-1}. MS (25 eV) *m*/*z* (relative intensity/%): 350 (M^+, 33), 272 (100, M^+ − FN), 271 (22), 270 (13), 243 (28), 181 (10). Anal. Calcd for $C_{24}H_{18}N_2O$: C, 82.26; H, 5.18; N, 7.99. Found: C, 81.99; H, 5.34; N, 7.94.

14a. Colorless powder (CH_2Cl_2−ether), mp 218−220 °C. ^{1}H NMR (200 MHz, $CDCl_3$): δ_{ppm} 2.6−3.2 (m, 4 H), 3.32 (s, 3 H), 3.96 (s, 3 H), 5.98 (s, 2 H), 7.2−7.6 (m, 10 H). ^{13}C NMR (50 MHz, $CDCl_3$): δ_{ppm} 28.0, 29.6, 54.0, 55.1, 57.8, 58.9, 83.6, 85.5, 113.4, 115.7, 126.4 (2 C), 126.7 (2 C), 128.1, 128.2, 128.8 (2 C), 128.9 (2 C), 130.4 (2 C), 132.0, 132.5, 138.8, 139.0, 161.1, 163.6. IR (KBr): ν 3450, 3050, 2950, 2850, 2250, 1760, 1680, 1630, 1600, 1575, 1495, 1445, 1435, 1360, 1240, 1190, 1160, 1140, 1115, 1075, 1050, 1025, 1010, 955, 935, 910 cm^{-1}. MS (70 eV) *m*/*z* (relative intensity/%): 466 (M^+, 8), 330 (25), 273 (24), 272 (100, M^+ − DMDCF), 271 (21), 270 (54), 243 (28), 241 (21), 165 (20), 163 (21), 91 (55). Anal. Calcd for $C_{28}H_{22}N_2O_5 \cdot (H_2O)_{0.67}$: C, 70.28; H, 4.92; N, 5.85. Found: C, 70.30; H, 4.84; N, 5.90.

exo-**15a.** Colorless powder (CH_2Cl_2−ether), mp 231−234 °C. ^{1}H NMR (200 MHz, $CDCl_3$): δ_{ppm} 2.6−3.0 (m, 4 H), 3.59 (s, 2 H), 5.63 (s, 2 H), 7.3−7.5 (m, 10 H). ^{13}C NMR (50 MHz, $CDCl_3$): δ_{ppm} 28.1 (2 C), 50.4 (2 C), 81.5 (2 C), 126.6 (4 C), 128.0 (2 C), 128.1 (2 C), 128.9 (4 C), 133.2 (2 C), 138.8 (2 C), 170.1 (2 C). IR (KBr): ν 3900 (br), 1875, 1840, 1785, 1670, 1620, 1595, 1570, 1490, 1440, 1365, 1300, 1245, 1230, 1210, 1170, 1155, 1075, 1040, 1025, 975, 940, 920, 890, 870, 855, 840, 820, 780, 755, 735 cm^{-1}. MS (70 eV) *m*/*z* (relative intensity/%): 371 (M^+ + 1, 23), 370 (M^+, 91), 273 (22), 272 (100, M^+ − MA), 243 (20). Anal. Calcd for $C_{24}H_{18}O_4 \cdot (H_2O)_{0.33}$: C, 76.58; H, 5.00. Found: C, 76.62; H, 5.03.

endo-**15a.** Colorless powder (CH_2Cl_2−ether), mp 247−249 °C. ^{1}H NMR (200 MHz, $CDCl_3$): δ_{ppm} 2.7−4.0 (m, 4 H), 3.94 (dd, J = 4.0, 2.3 Hz, 2 H), 5.67 (dd, J = 4.0, 2.3 Hz, 2 H), 7.3−7.5 (m, 10 H). ^{13}C NMR (50 MHz, $CDCl_3$): δ_{ppm} 28.5 (2 C), 52.5 (2 C), 79.1 (2 C), 126.4 (4 C), 127.9 (2 C), 128.6 (4 C), 130.4 (2 C), 131.4 (2 C), 139.1 (2 C), 167.9 (2 C). IR (KBr): ν 3450 (br), 1870, 1785, 1490, 1440, 1360, 1300, 1220, 1110, 1070, 1025, 980, 960, 930, 835, 810, 770 cm^{-1}. MS (70 eV) *m*/*z* (relative intensity/%): 371 (M^++ 1, 15), 370 (M^+, 56), 273 (22), 272 (100, M^+ − MA), 243 (24), 181 (12), 165 (19), 91 (12). Anal. Calcd for $C_{24}H_{18}O_4 \cdot (H_2O)_{0.25}$: C, 76.89; H, 4.97. Found: C, 76.93; H, 4.96.

trans-**16a.** Colorless needles (CH_2Cl_2−ether), mp 151−152 °C. ^{1}H NMR (200 MHz, $CDCl_3$): δ_{ppm} 2.5−2.6 (m, 4 H), 3.13 (s, 3 H), 3.53 (d, J = 4.8 Hz, 1 H), 3.70 (dd, J = 5.4, 4.8 Hz, 1 H), 3.79 (s, 3 H), 5.46 (s, 1 H), 5.78 (d, J = 5.4 Hz, 1 H), 7.3−7.5 (m, 10 H). ^{13}C NMR (50 MHz, $CDCl_3$): δ_{ppm} 27.2, 29.8, 50.0, 50.8, 51.5, 52.6, 79.1, 81.7, 125.6, 126.4 (2 C), 126.8 (2 C), 127.1, 127.3, 127.9, 128.4 (4 C), 133.5, 136.0, 139.7, 140.2, 170.3, 172.2. IR (KBr): ν 3450, 3050, 2950, 2850, 1745, 1735, 1595, 1495, 1430, 1365, 1320, 1305, 1075, 1015, 980, 900, 865, 820, 760, 700, 680 cm^{-1}. MS (70 eV) *m*/*z* (relative intensity/%): 417 (M^+ + 1, 14), 416 (M^+, 45), 273 (23), 272 (100, M^+ − DMF), 243 (22), 181 (12), 165 (15), 91 (15). Anal. Calcd for $C_{26}H_{24}O_5$: C, 74.98; H, 5.81. Found: C, 74.82; H, 5.86.

exo, *cis*-**16a.** Colorless needles (CH_2Cl_2−ether), mp 177−179 °C. ^{1}H NMR (200 MHz, $CDCl_3$): δ_{ppm} 2.5−3.0 (m, 4 H), 3.44 (s, 2 H), 3.75 (s, 6 H), 5.49 (s, 2 H), 7.2−7.5 (m, 10 H). ^{13}C NMR (50 MHz, $CDCl_3$): δ_{ppm} 28.1 (2 C), 51.3 (2 C), 52.4 (2 C), 80.3 (2 C), 125.8 (2 C), 126.7 (4 C), 127.4 (2 C), 128.6 (4 C), 135.8 (2 C), 139.5 (2 C),

(30) As one of the referee pointed out, it is not a good idea to judge the electronic state of **7**$^{\bullet\bullet}$, especially the singlet state ^{1}**7**$^{\bullet\bullet}$, with UDFT calculation, because these "singlet" species must be a mixture of singlet and triplet states (spin contamination). The most straightforward way to solve the problem of multiplicity may be an ESR study of **7**$^{\bullet\bullet}$ and a calculation study of **7**$^{\bullet\bullet}$ by uisng MP2, the complete active space SCF (CASSCF), or the perfect-pairing general valence bond (GVB-PP) method. These studies are now in progress and will be published elsewhere.

(31) (a) Maiti, A.; Gerken, J. B.; Masjedizadeh, M. R.; Mimieux, Y. S.; Little, R. D. *J. Org. Chem.* **2004**, *69*, 8574−8582. (b) Allan, A. K.; Carroll, G. L.; Little, R. D. *Eur. J. Org. Chem.* **1998**, 1−12. (c) Little, R. D. *Chem. Rev.* **1996**, *96*, 93−114. (d) Bregant, T. M.; Groppe, J.; Little, R. D. *J. Am. Chem. Soc.* **1994**, *116*, 3635−3636. (e) Jacobs, S. J.; Shultz, D. A.; Jain, R.; Novak, J.; Dougherty, D. A. *J. Am. Chem. Soc.* **1993**, *115*, 1744−1753. (f) Matsumoto, T.; Ishida, T.; Koga, N.; Iwamura, H. *J. Am. Chem. Soc.* **1992**, *114*, 9952−9959. (g) Dougherty, D. A. *Acc. Chem. Res.* **1991**, *24*, 88−94. (h) Trost, B. M. *Angew. Chem., Int. Ed. Engl.* **1986**, *25*, 1−20.

171.0 (2C). IR (KBr): ν 3450, 2950, 1755, 1730, 1595, 1495, 1440, 1360, 1330, 1215, 1190, 1170, 1055, 765, 745, 700 cm^{-1}. MS (70 eV) *m*/*z* (relative intensity/%): 416 (42, M^+), 273 (23), 272 (100, $M^+ -$ DMM), 243 (26), 165 (15), 91 (13). Anal. Calcd for $C_{26}H_{24}O_5$: C, 74.98; H, 5.81. Found: C, 74.69; H, 5.90.

endo, *cis*-**16a.** Colorless needles (CH_2Cl_2−ether), mp 176−179 °C. ^{1}H NMR (200 MHz, $CDCl_3$): δ_{ppm} 2.6−2.9 (m, 4 H), 3.33 (s, 6 H), 3.49 (dd, J = 3.2, 2.2 Hz, 2 H), 5.54 (dd, J = 3.2, 2.2 Hz, 2 H), 7.2−7.5 (m, 10 H). ^{13}C NMR (50 MHz, $CDCl_3$): δ_{ppm} 28.9 (2 C), 49.0 (2 C), 51.4 (2 C), 79.0 (2 C), 126.6 (4 C), 126.9 (2 C), 127.8 (2 C), 128.3 (4 C), 134.5 (2 C), 140.7 (2 C), 169.7 (2 C). IR (KBr): ν 3450, 2950, 1745, 1735, 1600, 1500, 1445, 1435, 1360, 1345, 1205, 1170, 775, 760, 700 cm^{-1}. MS (70 eV) *m*/*z* (relative intensity/%): 417 ($M^+ + 1$, 13), 416 (M^+, 41), 273 (18), 272 (100, $M^+ -$ DMM), 243 (22), 181 (10), 165 (16), 91 (16). Anal. Calcd for $C_{26}H_{24}O_5$: C, 74.98; H, 5.81. Found: C, 74.71; H, 5.83.

Measurement of Time-Resolved Absorption Spectra on LFP. Nanosecond time-resolved absorption spectroscopy upon LFP was carried out with a pulsed YAG laser (Continuum Surelite-10, Nd, THG, λ_{ex} = 355 nm, 55 mJ) and a Xe arc lamp (150 W) as the monitoring light. [**6a**] = 25 mM, [DCA] = [$NMQ^+BF_4^-$] = 1.0 mM, [toluene] = 2.0 M. For the details, see ref 11.

Quantum Chemical Calculations. The geometries of the radical cations and biradicals were optimized at the unrestricted B3LYP level with the standard cc-pVDZ basis set. Vibrational analyses confirmed a DFT stationary point as energy minima (no imaginary frequencies). Wavefunction analyses for charge and spin distributions used the conventional Mulliken partitioning scheme.[32] Spin contamination is negligible for **6a**$^{\bullet+}$, **6b**$^{\bullet+}$, **7a**$^{\bullet+}$, and **7b**$^{\bullet+}$ (S^2 = 0.7501−0.7503), and for ^{3}**7a**$^{\bullet\bullet}$ and ^{3}**7b**$^{\bullet\bullet}$ (S^2 = 2.0011−2.0012), but not for ^{1}**7a**$^{\bullet\bullet}$ and ^{1}**7b**$^{\bullet\bullet}$ (S^2 = 0.3716−0.3767). Application of MP2, the complete active space SCF (CASSCF), and the perfect-pairing general valence bond (GVB-PP) calculation to ^{1}**7a**$^{\bullet\bullet}$ and ^{1}**7b**$^{\bullet\bullet}$ are now in progress and will be published elsewhere. Excitation energies were computed using time-dependent density functional theory of the B3LYP level (TD-B3LYP) with the cc-pVDZ basis set. DFT calculations for them were carried out with the Gaussian 98 programs[23] using extended basis sets, including d-type polarization functions on carbon.

Acknowledgment. H.I., K.M., and S.T.-K. gratefully acknowledge financial support in the form of a Grant-in-Aid for Scientific Research on Priority Areas (Area No. 417) and others (Nos. 16655018, 18037063, and 19350025) from the Ministry of Education, Culture, Sports, Science, and Technology of Japan. H.I. thanks financial support by the Japan Science and Technology Agency for Research for Promoting Technological Seeds, the Izumi Science and Technology Foundation, the Shorai Foundation, the Iketani Foundation for Science and Technology, and the Mazda Foundation. T.I. gratefully acknowledges financial support by the Sasakawa Scientific Research Grant from the Japan Science Society. We also thank Professor Emeritus T. Miyashi (Tohoku University) and Professors S. Koseki and T. Asada (Osaka Prefecture University) for enlightening discussions.

Supporting Information Available: Complete ref 23, DFT calculation results, and an energy diagram for the PET reaction of **6a**, and ^{1}H and ^{13}C NMR spectra of new compounds (**6**, **9**, and **14**−**16**). This material is available free of charge via the Internet at http://pubs.acs.org.

JA074000B

(32) Mulliken, R. S. *J. Chem. Phys.* **1955**, *23*, 1833−1840.